Studies of the Crystalline–Liquid Crystalline Phase Transition of Lipid Model Membranes. II. Analysis of Electron Spin Resonance Spectra of Steroid Labels Incorporated into Lipid Membranes

E. Sackmann* and H. Träuble

Contribution from the Max-Planck-Institut für Biophysikalische Chemie, 34 Göttingen, Nikolausberg, Germany. *Received August 27, 1971*

Abstract: Esr spectra of androstane spin labels incorporated into dipalmitoyllecithin model membranes were measured as a function of temperature and label concentration in part I of this series. These spectra are analyzed in the present paper by computer simulation. The spectra measured at low label concentration (negligible radical interaction) can be simulated by a superposition of three Lorentzian lines of different line widths. The crystalline–liquid crystalline phase transition of the lipid material is indicated by a sharp decrease of the line width with increasing temperature. It was shown in part I that increasing label concentration produces broadened esr spectra. These spectra can be analyzed in terms of magnetic interactions between the radicals (dipole–dipole and spin-exchange interaction). Three methods were used to simulate the spectra. First we took into account the exchange interaction and second the dipole–dipole interaction; in a third approach these two effects were combined. It is demonstrated by the computer analysis that the line broadening observed with increasing label concentration is determined mainly by the exchange interaction which is characterized by the rate of exchange W_{ex} between the radicals. The lipid-phase transition produces a sharp decrease of W_{ex} with increasing temperature at about 35°. This temperature dependence is in complete contrast to the behavior of free radicals in solution and suggests a structural change of the steroid–lecithin system at the phase transition. Different functional dependencies of W_{ex} on the molar ratio c label:lipid are observed at temperatures below and above the phase transition. Above T_t the exchange frequency W_{ex} increases linearly in c, whereas below T_t the exchange frequency is a linear function of $1/\sqrt{c}$ which is proportional to the average label separation d_{la}. An explanation for these findings is given in an accompanying paper, part III of this series.

1. Introduction

In a previous paper[1] (part I of this series) we reported experimental studies of the crystalline–liquid crystalline phase transition of dipalmitoyllecithin model membranes with a characteristic transition temperature of $T_t \approx 41°$. Two groups of experiments were performed to study the conformational changes of the lipid membranes at the phase transition.

(a) Optical measurements were performed using 8-anilino-1-naphthalene sulfonate (ANS) as a conformational sensitive fluorescence probe. Bromthymol Blue (BTB) was used as a conformational sensitive absorption probe. These probes can be used to indicate changes in the polar head group arrangement of the lipid structure at the crystalline–liquid crystalline phase transition.

(b) The spin label technique was applied to study conformational changes within the hydrophobic region of the membrane. An *N*-oxyl-4′,4′-dimethyloxazolidine derivative of 5α-androstan-3-one-17β-ol was used as the spin label. The chemical structure of this molecule is shown in Figure 1. The paramagnetic center is the nitroxide group carrying an unpaired electron in a $2p\pi$ orbital centered at the nitrogen nucleus. Hubbell and McConnell[2] have provided evidence that this label is intercalated between the hydrocarbon chains of the lipid molecules with the OH group oriented toward the polar phase. Since the oxazolidine ring is rigidly bound to the steroid nucleus, a rotation of the nitroxide group reveals a rotation of the whole molecules.

The primary goal of our esr measurements was to study the possible influence of the crystalline–liquid crystalline phase transition on the organization of mixed steroid–lecithin model membranes. We have used the magnetic interaction between the steroid label molecules as a structure-sensitive parameter. The information about this interaction is contained in the shape of the esr spectra. The data required for the development of a theoretical model are provided by measurements of the temperature and concentration dependence of the esr line shape. Five samples with label:lipid molar ratios c ranging from $c = 0.01$ to $c = 0.27$ were studied in the temperature range between 18 and 55°.

At low label concentrations ($c \leq 0.01$) the interaction between the radicals is negligible and clearly resolved triplet spectra are observed. When the label concentration increases the spectra for $T < T_t$ gradually coalesce into broad one-line spectra (*cf.* Figure 7, part I). Upon heating the system above T_t these one-line spectra are resolved into triplet spectra.

The present paper is dedicated to the quantitative analysis of the esr measurements presented in part I by computer simulation. It will be shown that for low label concentrations (no interaction) the spectra can be simulated by a superposition of three Lorentzian lines. The broadening observed with increasing label concentration (*cf.* Figure 7, part I) is a result of the increasing interactions between the radicals. In the computer simulation of these spectra two interaction mechanisms will be taken into account: the exchange interaction and the magnetic dipole–dipole interaction.

(1) Part I: E. Sackmann and H. Träuble, *J. Amer. Chem. Soc.*, **94**, 4482 (1972).
(2) W. L. Hubbell and H. M. McConnell, *Proc. Nat. Acad. Sci. U. S.*, **61**, 12 (1968); **63**, 16 (1969).

2. Basic Principles

The paramagnetic resonance spectrum of a system of interacting spin labels can be described theoretically by the following spin Hamiltonian[3,4]

$$\mathcal{H} = |\beta|\mathbf{S}\cdot\mathbf{g}\cdot\boldsymbol{H}_0 + h\mathbf{S}\cdot\mathbf{T}\cdot\boldsymbol{I} - \beta_N\boldsymbol{I}\cdot\mathbf{g}_N\cdot\boldsymbol{H}_0 + \mathcal{H}(\text{exchange}) + \mathcal{H}(\text{dipole}) \quad (1)$$

The first and the third term in this expression describe the action of the applied field $\boldsymbol{H}_0$ on the electron spin angular momentum $\boldsymbol{S}$ and the nuclear spin angular momentum $\boldsymbol{I}$. The second term represents the electron-nuclear hyperfine coupling characterized by the nuclear hyperfine tensor $\mathbf{T}$. $\mathbf{g}$ and $\mathbf{g}_N$ are the g-factor tensors of the electron and of the ^{14}N nucleus; β and β_N denote the electron and the nuclear Bohr magnetons, respectively. The terms abbreviated by $\mathcal{H}$(exchange) and $\mathcal{H}$(dipole) denote the Hamiltonians of the exchange and the dipole–dipole interaction, respectively. The first three terms in eq 1 describe the esr spectra of dilute radical solutions without interactions.[3–5]

In the coordinate system adopted in Figure 1 the g and T tensors of the androstane label have the following components[5]

$$(T_x, T_y, T_z) = (5.8, 5.8, 30.8 \pm 0.5)\ \text{G}^{6} \quad (2)$$

$$(g_x, g_y, g_z) = (2.0089, 2.0058, 2.0021 \pm 0.001)\ \text{G}^{6}$$

In the case of very rapid tumbling of the spin labels ($\tau \leq 10^{-10}$ sec), the anisotropy of the T tensor is averaged out and the hyperfine coupling term in eq 1 is reduced to $ha_H\boldsymbol{I}\cdot\boldsymbol{S}$, where the hyperfine coupling constant a_H is given by

$$a_H = {}^1/_3(T_x + T_y + T_z) = 14.1\ \text{G} \quad (3)$$

The interaction terms $\mathcal{H}$(exchange) and $\mathcal{H}$(dipole) in eq 1 can be expressed in the following way.[7]

(2a) Exchange Interaction. For an ensemble of electron spins ($\boldsymbol{S}_i$) the Hamiltonian of the exchange interaction is given by[7]

$$\mathcal{H}(\text{exchange}) = -2\sum_{i<j} J_{ij}\boldsymbol{S}_i\cdot\boldsymbol{S}_j \quad (4)$$

where J_{ij} is the exchange integral for two interacting radicals i and j. J_{ij} can be expressed in terms of the wave functions Ψ_i and Ψ_j of the unpaired electrons i and j as

$$J_{ij} = \int \Psi_i(i)\Psi_j(j)(e^2/|r_{ij}|)\Psi_i(j)\Psi_j(i)\,d\tau_i d\tau_j \quad (5)$$

In this expression $|r_{ij}|$ is the distance between the electrons i and j. The value of J_{ij} depends on the overlap between the two wave functions Ψ_i and Ψ_j and falls off very rapidly with increasing distance between the radicals. Therefore it is customary (*cf.* ref 7) to consider exchange interaction between nearest neighbors only and to replace the exchange integral J_{ij} by an average value J.

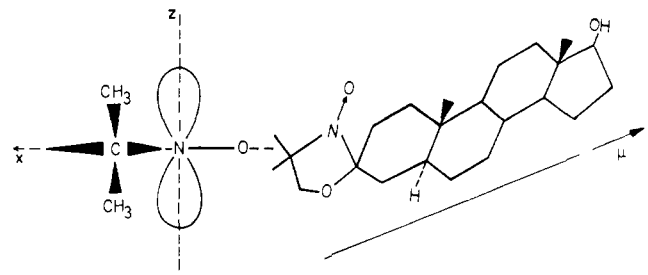

Figure 1. Structure of the steroid spin label. Right side: chemical structure of the *N*-oxyl-4′,4′-dimethyloxazolidine derivative of 5α-androstan-3-one-17β-ol. The unpaired electron is located at the nitrogen atom of the N–O group in a $2p\pi$ orbital. Left side: definition of the principal axis system of the hyperfine coupling tensor $\mathbf{T}$, assuming planarity of the oxazolidine ring. The long axis of the $2p\pi$ orbital is perpendicular to the long axis of the steroid molecule (μ axis).

The exchange interaction $\mathcal{H}$(exchange) leads to an exchange of the spin states of two interacting radicals and thus induces flip-flops between oppositely oriented spins. As a quantitative measure of the exchange coupling we will use the exchange frequency W_{ex}. For immobilized radicals W_{ex} is given by[7,8]

$$W_{ex} = J/h \quad (6)$$

For dilute liquid solutions of radicals the exchange process is diffusion-controlled and thus depends on the solvent viscosity η.[7,9,10]

The effect of the exchange interaction on a multiplet esr spectrum consists in a line broadening in the case of "weak exchange" and in a line narrowing in the case of "strong exchange.[8] In the case of a triplet spectrum the exchange interaction leads to the following effects.

"Weak Exchange" (Exchange Broadening). At low label concentrations the exchange interaction leads to a broadening of all three lines. Simultaneously the two side bands move to the center of the spectrum. The additional broadening of an individual line due to exchange interaction is given by $\Delta\nu_{ex} = 2W_{ex}$; hereby the line width is defined as the frequency difference between the maximum and the minimum of a line of the first derivative esr spectrum. This broadening effect predominates as long as the separation of the lines given by a_H (MHz) is large compared to W_{ex}. When a_H becomes equal to W_{ex} the individual lines coalesce into one broad line.

"Strong Exchange" (Exchange Narrowing). When the exchange frequency is large compared to the value of the line separation ($W_{ex} \gg a_H$), the width of the collapsed line decreases with increasing exchange frequency W_{ex}. The resulting line is of the Lorentzian type and has a line width of $(a_H)^2/W_{ex}$.

(2b) Dipole–Dipole Interaction. The magnetic dipole–dipole interaction of an electron spin $\boldsymbol{S}_i$ with the other spins $\boldsymbol{S}_k$ of the spin system is given approximately by (*cf.* Pake[7])

$$\mathcal{H}(\text{dipole}) = g^2\beta^2\sum_{k\neq i}|r_{ik}|^{-3}(3\cos^2\theta_{ik} - 1)\times(\boldsymbol{S}_i\boldsymbol{S}_k - 3S_{z,i}S_{z,k}) \quad (7)$$

(3) H. M. McConnell and B. G. McFarland, *Quart. Rev. Biophys.*, **3**, 91 (1970).
(4) O. H. Griffith and A. S. Waggoner, *Accounts Chem. Res.*, **2**, 17 (1969).
(5) W. L. Hubbell and H. M. McConnell, *J. Amer. Chem. Soc.*, **93**, 314 (1971).
(6) A value of 1 G of the external field corresponds to a precession frequency of 2.8 MHz.
(7) G. E. Pake, "Paramagnetic Resonance," W. A. Benjamin, New York, N. Y., 1962.
(8) P. W. Anderson, *J. Phys. Soc. Jap.*, **9**, 316 (1954).
(9) G. E. Pake and T. R. Tuttle, *Phys. Rev. Lett.*, **3**, 423 (1959).
(10) W. Plachy and D. Kivelson, *J. Chem. Phys.*, **47**, 3312 (1967).

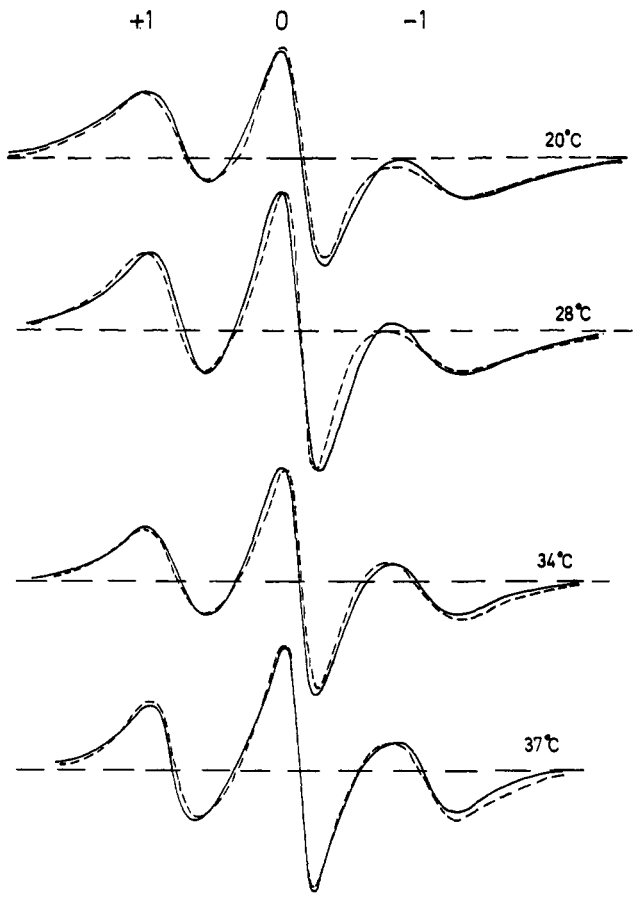

Figure 2. First-derivative esr spectra of androstane labels incorporated into lipid monolayer vesicles. Low label concentration. The label to lipid molar ratio was $c = 0.01$, corresponding to an average next-nearest-neighbor distance $d_{1a} \approx 75$ Å between the label molecules; (—) measured spectra; (---) computer simulated spectra. The spectra were simulated by superposition of Lorentzian lines positioned at $H_0 - a_H$, H_0, $H_0 + a_H$. The values of the line widths are given in Table I. Excellent agreement between calculated and measured spectra is obtained. The notations (−1), (0), (+1) give the respective magnetic quantum numbers of the nitrogen nuclear spin.

In this equation g is the g factor of the unpaired electrons and β is the electron Bohr magneton. θ_{ik} denotes the angle between the external magnetic field vector H_0 and the vector r_{ik} connecting the spins S_i and $S_k \cdot S_z$ is the z component of the electron spin angular momentum operator. It has been shown by Van Vleck[11] that the effect of the dipole–dipole interaction on the esr spectra of an ensemble of spins consists in a line broadening. This effect can be understood qualitatively as follows. The magnetic moments of the radicals k produce a resulting local field H_d at the site of the radical i which is superimposed on the external field H_0. In a system of immobilized and statistically distributed radicals the field H_d fluctuates due to fluctuations in the angles θ_{ik} and the distances $|r_{ik}|$. This leads to a resulting resonance field $H_0 + H_d$ which fluctuates from radical to radical and produces a broadening of the spectrum. The Hamiltonian eq 7 was applied by Van Vleck to the problem of the dipolar broadening of esr spectra of spin systems. The following mean square value of the local magnetic field is obtained.

(11) J. H. Van Vleck, *Phys. Rev.*, **52**, 1178 (1937).

$$\langle H_d^2 \rangle = {}^9/_{16} \sum_k g^2\beta^2 |r_{ik}|^{-6} (3 \cos^2 \theta_{ik} - 1)^2 \quad (8)$$

This value is a measure of the line width ΔH_d (in gauss) of a dipolar-broadened line. For the first derivative of a Gaussian line the following relation is valid.

$$\Delta H_d = \sqrt{\langle H_d^2 \rangle} \quad (9)$$

For a Lorentzian line there exists no simple relationship between the line width ΔH_d and $\langle H_d^2 \rangle$.

The value of ΔH_d can be estimated from eq 8 when it is assumed that the label molecules are distributed statistically within a lipid lattice. Denoting with d_{1a} the average distance between the radicals and assuming a triangular lattice we find with $g = 2$

$$\Delta H_d = 3 \times 10^4 (1/d_{1a})^3 \quad (d_{1a} (= d_{label}) \text{ in Å}) \quad (10)$$

The dipolar broadening is reduced when the label molecules perform tumbling motions because in this case the field H_d is partially averaged out. It was shown by Kivelson[12] that the line broadening due to dipole–dipole interactions can be calculated to a good approximation if the correlation time τ of the molecular tumbling is very small ($\tau \leq 10^{-10}$ sec). For larger τ values the line broadening cannot be determined easily.

3. Computer Simulation of the Esr Spectra

3.1. Low Label Concentration (Negligible Interaction). In Figure 2 we have replotted the esr spectra of Figure 5, part I. These spectra were measured at a label concentration of $c = 0.01$ between 20 and 52°. The spectra are nearly symmetric triplet spectra. This indicates a fast and almost isotropic tumbling of the label molecules both above and below T_t.[13]

Values of the correlation time τ characterizing the molecular tumbling rate can be estimated by comparison of the measured spectra with theoretical spectra calculated by Itzkowitz[14] and Alexandrov, *et al.*[15] These authors treated the tumbling motion of the label molecules as an angular random walk problem. From this comparison we estimate a correlation time of $\tau = 10^{-8}$ sec at 20°.

It turns out that the measured spectra can be simulated by a superposition of three Lorentzian lines centered at $(H_0 - a_H)$, (H_0), and $(H_0 + a_H)$ with different values of the line width. As demonstrated by Figure 2, excellent agreement between the measured and calculated spectra is obtained by this procedure. The values of the line widths $\Delta H_0(+1)$, $\Delta H_0(0)$, and $\Delta H_0(-1)$ are summarized in Table I. These values

Table I. Temperature Dependence of the Line Widths ΔH_0 (in gauss) of the Three Lines (+1, 0, −1) of Esr Spectra Observed in the Absence of Radical Interaction[a]

T, °C	20	28	34	37	41	52
$\Delta H_0(+1)$	9.5	8.5	8.1	7.2	5.0	4.3
$\Delta H_0(0)$	6.3	5.7	4.5	4.0	3.8	3.4
$\Delta H_0(-1)$	13.0	12.0	9.1	5.7	6.4	4.8

[a] These values were determined by computer simulation of measured esr spectra shown in Figure 2.

(12) D. Kivelson, *J. Chem. Phys.*, **27**, 1087 (1957); **33**, 1094 (1960).
(13) The effective tumbling motion may contain also contributions from the rotational motion of the vesicles.
(14) M. Itzkowitz, *J. Chem. Phys.*, **46**, 3048 (1967).
(15) I. V. Alexandrov, A. N. Ivanova, N. N. Korst, A. V. Lazarev, A. I. Prikhozhenko, and V. B. Stryukov, *Mol. Phys.*, **18**, 681 (1970).

compare fairly well with the values determined empirically in part I (*cf.* Figure 6, part I), where the line width was defined as the distance in gauss between the maximum and minimum of each line of the first derivative spectra. The computer calculated values exhibit the same sharp decrease at the phase transition as the values determined empirically from Figure 5, part I (*cf.* Figure 6, I). This confirms that the phase transition produces an abrupt increase in the rotational freedom of the label molecules. The decrease in line width by a factor of 2–3 (*cf.* Figure 6, part I, and Table I) observed upon heating the system above T_t corresponds to a decrease of the correlation time τ by the same factor.[7,12]

3.2. High Label Concentration (Radical Interactions). As demonstrated by Figure 7, part I, the esr spectra become fairly complicated when the label concentration exceeds a critical value characteristic for the onset of interactions between the radicals ($c \gtrsim 0.02$). To analyze these spectra in terms of the dipole–dipole interaction and the exchange interaction, we have used three computer programs in which these two mechanisms were treated separately, (a), (b), and in combination (c).

(a) Exchange Interaction. The influence of the exchange interaction on the esr spectra can be calculated using the random jump model by Anderson[8] or by solving the Bloch equation modified by appropriate exchange terms. In a rotating coordinate system the modified Bloch equation has the following form[16,17]

$$\frac{dG_j}{dt} + \left(\frac{1}{T_{2j}^0} - i(\omega_j - \omega)\right)G_j - \sum_{k=1}^{3}\left(\frac{G_k}{\tau_{jk}} - \frac{G_j}{\tau_{kj}}\right) = ig\beta H_1 M_{0j} \quad (11)$$

In this equation G_j denotes the complex magnetic moment of the spin system in a direction perpendicular to the external magnetic field H_0. The index j refers to the three possible quantum numbers $(+1, 0, -1)$ of the nitrogen nuclear spin. G_j may be written as $G_j = u_j + iv_j$ where u_j is the component of the magnetic moment parallel to the rotating component of the microwave field H_1, and v_j is the component of G_j perpendicular to this rotating component. ω denotes the Larmor frequency[18] corresponding to the value of the variable applied magnetic field; ω_j denotes the Larmor frequency corresponding to the position of the three triplet lines; ω_j can take on the following three values

$$\omega_0 - (g\beta/\hbar)a_H;\ \omega_0;\ \omega_0 + (g\beta/\hbar)a_H \quad (12)$$

where ω_0 determines the position of the center of the spectrum; ω_0 can be taken equal to zero in the following discussion.

In eq 11 the quantity M_{0j} denotes the value of the static magnetization of the spin system in a direction parallel to the external field H_0. $1/\tau_{jk}$ and $1/\tau_{kj}$ are the rates of the spin exchange between molecules with nitrogen nuclear spin components I_{zj} and I_{zk}. T_{2j}^0 is the transverse relaxation time for the jth component in the absence of exchange interaction. For a first-derivative Lorentzian line T_{2j} is connected with the line width ΔH_j according to

$$\Delta H_j = \frac{\hbar}{g\beta}\frac{2}{\sqrt{3}T_{2j}} \quad (13)$$

The line width ΔH_j is defined as the distance in gauss between the maximum and the minimum of each line. We have solved eq 11 assuming

$$\tau_{jk} = \tau_{kj} = \tau \quad (14)$$

where $1/\tau$ is identical with the exchange frequency W_{ex}. The spectra were recorded with a sweep rate low enough to guarantee steady state conditions: $dG_j/dt = 0$ ("slow passage"). Under these conditions eq 11 leads to the following two equations for the real and imaginary parts (u_j and v_j) of G_j.

$$u_j\left[\frac{1}{T_{2j}} + 3W_{ex}\right] - W_{ex}\sum_{k=1}^{3}u_k + (\omega_j - \omega)v_j = 0 \quad (15)$$

$$v_j\left[\frac{1}{T_{2j}} + 3W_{ex}\right] - W_{ex}\sum_{k=1}^{3}v_k - (\omega_j - \omega)u_j = -P_j \quad (16)$$

P_j is proportional to $g\beta H_1 M_{0j}$ and measures the fraction of radicals with a nitrogen nuclear spin component I_{zj}. The statistical weights of the three spin states of the nitrogen nucleus are identical and therefore the value of P_j is independent of j ($P_j = P$). The three components u_j can be eliminated from eq 16 using eq 15. This leads to a set of three equations for the components v_j. From these equations we have calculated the components v_j as a function of ω using a PDP-8I computer. The total line shape of the esr absorption spectra is proportional to

$$V(\omega) = v_{+1}(\omega) + v_0(\omega) + v_{-1}(\omega) \quad (17)$$

The first derivative of this expression is compared with the experimental spectra. To produce optimal fit with the experimental spectra, eq 15 and 16 were solved with varying values of W_{ex}. Thereby the values of

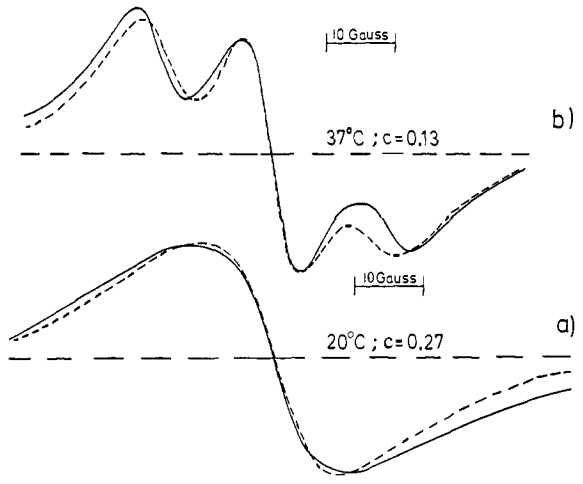

Figure 3. Comparison between experimental (—) and computer simulated spectra (---). The spectra were calculated with a modified Bloch equation assuming exchange interaction only. The overall shape and much of the fine structure of the experimental spectra are reproduced. Optimal fit is obtained with the values $W_{ex} = 12.0$ MHz for the spectrum in Figure 3a ($c = 0.27$, $T = 20°$) and $W_{ex} = 7.5$ MHz for the spectrum in Figure 3b ($c = 0.13$, $T = 37°$).

(16) H. M. McConnell, *J. Chem. Phys.*, **28**, 430 (1958).
(17) C. S. Johnson, *Mol. Phys.*, **1**, 25 (1967).
(18) The Larmor frequency ω and the value of the external magnetic field H are related by $\omega = g\beta/\hbar H$. For $g = 2.0023$, $\omega = 17.6087 \times 10^6$ Hz.

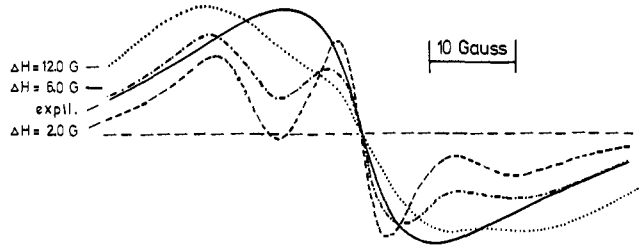

Figure 4. Comparison of a measured esr spectrum (preparation e, $c = 0.27$, $T = 20°$) with theoretical spectra calculated on the basis of dipolar broadening only. For ΔH_{0j} in eq 18 we have taken the values given in Table I. Three values of the dipolar broadening ΔH_d were tested: $\Delta H_d = 2.0$ G (---); $\Delta H_d = 6.0$ G (-·-·-); $\Delta H_d = 12.0$ (· · ·). Agreement between theoretical and experimental spectra cannot be obtained.

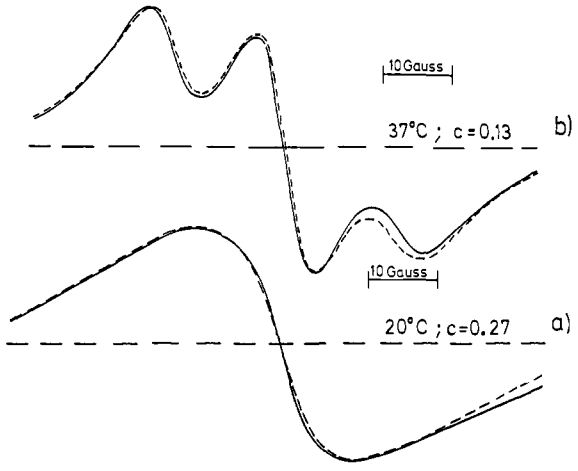

Figure 5. Comparison between experimental spectra (—) and theoretical spectra (---). The spectra were calculated with a modified Bloch equation taking into account both exchange interactions and dipolar interactions between the radicals. The experimental curves are the same as in Figure 3. Very good fit is obtained with $W_{ex} = 10.5$ MHz for the spectrum in Figure 5a ($c = 0.27$, $T = 20°$) and $W_{ex} = 6.0$ MHz for the spectrum in Figure 5b ($c = 0.13$, $T = 37°$). $\Delta H_0 = 1.0$ G in both cases.

T_{2j}^0 were adapted from the spectra without radical interactions (*cf.* Table I).

A comparison between the theoretical and the measured spectra is presented in Figure 3 for two label concentrations and different temperatures. At high label concentration ($c = 0.27$) and for $T = 20°$ the measured spectrum consists of a single broad line (*cf.* Figure 3a). At somewhat lower label concentration ($c = 0.13$) and for $T = 37°$ the spectrum shows some fine structure (*cf.* Figure 3b).

As can be seen from Figure 3a very good fit is obtained between the calculated and the measured spectra in the central region. In the outer regions the theoretical curves fall off more rapidly. In the spectrum of Figure 3b again very good fit is obtained in the central region of the spectrum. The calculated and the measured spectra differ, however, in the position of the maxima and minima of the side bands.

(b) Dipole–Dipole Interaction. As mentioned in section 2b the dipole–dipole interaction leads to a broadening of the triplet lines. We have studied this effect in more detail by attributing a dipolar broadening ΔH_d to each line. The resulting effective line widths are then

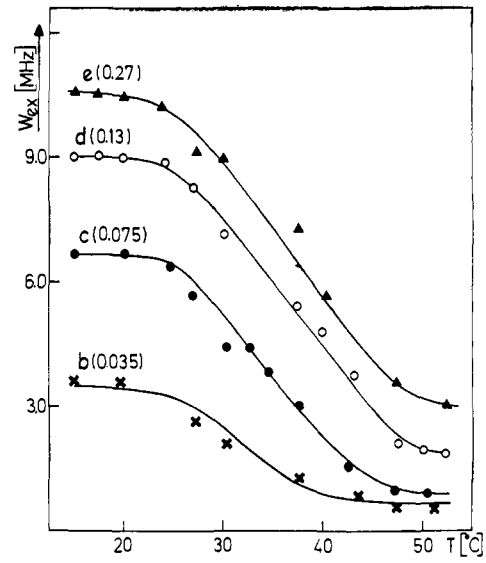

Figure 6. Temperature dependence of the exchange frequency W_{ex} determined by fitting calculated esr spectra to the experimental spectra presented in Figure 7, part I. In the calculation both the exchange interaction and the dipolar interaction between the radicals were taken into account. (Notation: letter = number of preparation, brackets = molar ratio label:lipid). The transition curves seem to consist of two stages: a "pretransition" at about 30° and a main transition at about 40°. The "pretransition" may be attributed to a substantial increase in the rotational freedom of the radicals, whereas the main transition involves conformational changes within the hydrocarbon chains (*cf.* part III, Discussion).

$$\Delta H_j = \Delta H_{0j} + \Delta H_d \qquad (18)$$

where ΔH_{0j} denotes the line width in the absence of interaction (*cf.* Table I).

Using eq 18 new T_{2j} values were calculated according to eq 13 and a computer simulation was performed as above. Typical results are shown in Figure 4 for three values of ΔH_d ($\Delta H_d = 2.0$, 6.0, and 12.0 G). Increasing dipolar interaction produces a gradual broadening of the lines and a shift of the maxima of the side bands away from the center. Satisfactory fit between calculated and measured spectra cannot be obtained. This is seen most clearly when calculated spectra are compared with spectra measured at high label concentration (*cf.* Figure 4).

(c) Dipole–Dipole and Exchange Interaction. The experimental spectra can be simulated almost exactly when a small dipolar broadening is taken into account in addition to the exchange interaction. For this purpose we have replaced the value of $1/T_{2j}^0$ in eq 11 by

$$1/T_{2j}^1 = 1/T_{2j}^0 + 1/T_2^d \qquad (19)$$

where $1/T_2^d$ describes the dipolar line broadening. The corresponding value of ΔH_d can be obtained from eq 13. In the computer simulation now both parameters, ΔH_d and W_{ex}, were varied to produce optimal fit. As can be seen from Figure 5 excellent agreement with the measured spectra is obtained. Comparison of Figure 3 and Figure 5 shows that the shape of the broadened spectra is determined mainly by the exchange interaction. The values of W_{ex} calculated by the "combined" procedure differ from those obtained with the exchange model by not more than 20%. The calculated values of ΔH_d and W_{ex} are presented in Table II and in Figure 6, respectively. The accuracy of these

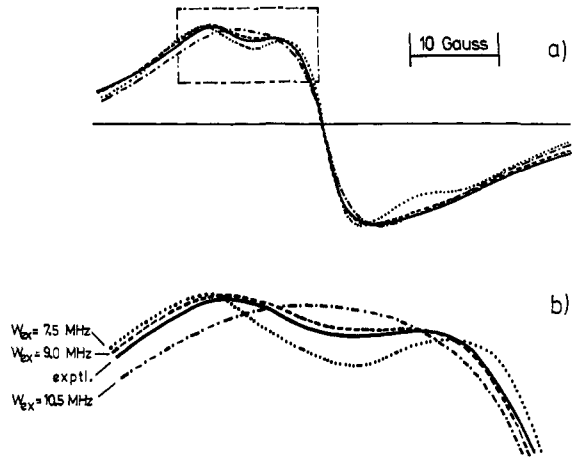

Figure 7. Dependence of the line shape of calculated esr spectra on the exchange interaction W_{ex} for constant dipolar interaction (ΔH_d = 1.0 G). Part of Figure 7a is shown on an enlargened scale in Figure 7b. The values of W_{ex} are W_{ex} = 7.5 MHz (···); W_{ex} = 9.0 MHz (---); W_{ex} = 10.5 MHz (-·-·). The experimental spectrum (—) was measured at T = 27° for a label:lipid molar ratio c = 0.27.

values may be judged from Figure 7 which demonstrates the influence of the value of W_{ex} on the shape of the spectra at constant dipolar interaction. The uncertainty of the calculated W_{ex} values is less than 10%.

Table II. Dipolar Line Broadening ΔH_d (in gauss)[a] for Different Temperatures and Label:Lipid Molar Ratios c

Prepn	15°	20°	27°	30°	37°	50°
b (c = 0.035)	0.0	0.0	0.0	0.0	0.0	0.0
c (c = 0.075)	0.5	0.0	0.0	0.0	0.0	0.0
d (c = 0.13)	1.5	1.0	1.0	1.0	1.0	0.0
e (c = 0.27)	2.0	1.5	1.0	1.0	1.0	0.0

[a] These values were determined by computer simulation of the spectra presented in Figure 7, part I.

4. Discussion

For the interpretation of the esr spectra it is important to know if the steroid molecules are incorporated quantitatively into the lipid matrix or if part of the label molecules are dissolved in the inner organic phase of the vesicles (*cf.* Figure 3, part I) or in the outer aqueous phase. The following arguments are relevant to this question.

1. Dilute solutions of the androstane spin label in organic solvents exhibit very sharp symmetric triplet spectra of the type shown in Figure 8a. For higher concentrations exchange-broadened spectra are observed which show a characteristic temperature dependence corresponding to $W_{ex} \propto T/\eta$[9,10] where η denotes the solvent viscosity. As is seen in Figure 2 the spectra of the androstane–lecithin system with low label concentration differ substantially from the spectrum in Figure 8a.

On the original records there are indications that a low-intensity spectrum of the type shown in Figure 8a is superimposed on the main spectrum. The intensity of these lines is, however, so low that not more than about one-hundredth of the total steroid content can be dissolved in the inner organic phase of the vesicles. For higher label concentrations the same must be true

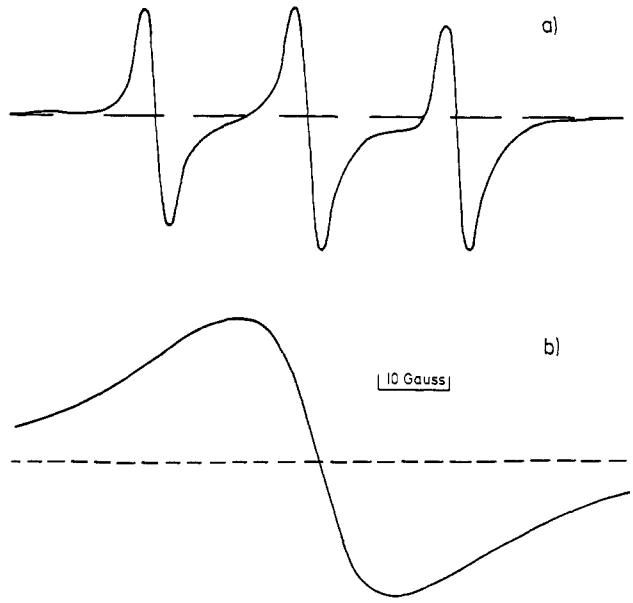

Figure 8. (a) First-derivative esr spectrum of the androstane label dissolved in chloroform; 10^{-3} mol/l. A very sharp triplet spectrum is observed. (b) Spectrum of an aqueous dispersion of the androstane label; 10^{-2} mol/l.

because in this case we observe a sharp decrease in the exchange frequency W_{ex} with increasing temperature in complete contrast to the behavior expected for solutions of androstane molecules in organic solvents.

2. We must consider the possibility that label molecules may be dissolved (or dispersed) in the aqueous phase. Figure 8b shows an esr spectrum of a dispersion of androstane molecules in water. A very broad one-line spectrum is observed at all temperatures for concentrations larger than 10^{-5} mol/l. In our preparations the label concentration ranged between 0.05 and 2 × 10^{-3} mol/l. with respect to the water content; thus the label concentration was far above the solubility limit of the steroid molecules in water (10^{-5}–10^{-6} mol/l.). Spectra similar to the one in Figure 8b were observed only at very high label concentrations. However, these spectra depend very sensitively upon temperature (*cf.* Figure 7.4, part I) and therefore cannot be attributed to steroid molecules dispersed in the aqueous phase.

The sharp increase in the exchange frequency W_{ex} upon lowering the temperature from $T > T_t$ to $T < T_t$ (*cf.* Figure 6) might be taken to indicate a complete separation of the steroid molecules from the lipid matrix upon lowering the temperature. According to Figure 8b this process would indeed produce a line broadening. However, this mechanism should result in considerable irreversible effects when the temperature is cycled between $T > T_t$ and $T < T_t$. In contrast, changes in the esr line shape at the phase transition are completely reversible. We conclude from these considerations that the observed changes in the esr spectra at the phase transition must be due to changes in the internal organization of the mixed steroid–lecithin system.

In part III of this series a theoretical model will be developed for the structure of the steroid-in-lecithin system for $T > T_t$ and $T < T_t$. Use will be made of the concentration dependence and the temperature dependence of W_{ex}. These two functional dependencies

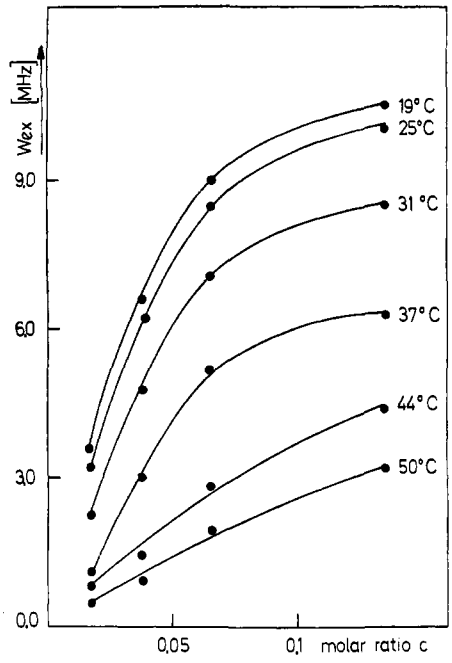

Figure 9. Concentration dependence of the exchange frequency W_{ex} at different temperatures. W_{ex} is plotted against c, the molar ratio label:lipid. A nearly linear increase of W_{ex} with c is found at temperatures above the phase transition (T = 44, 50°).

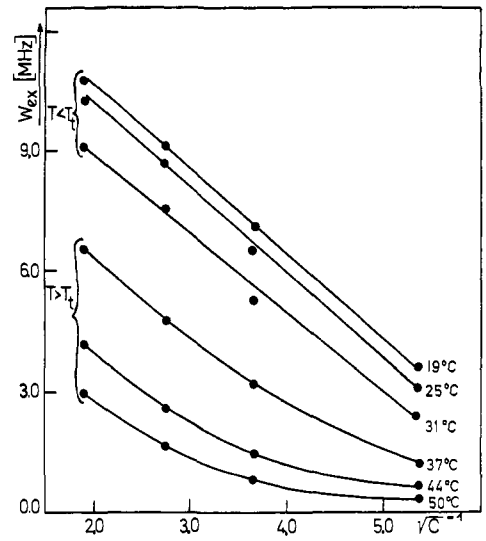

Figure 10. Concentration dependence of the exchange frequency W_{ex} at different temperatures. The W_{ex} values of Figure 9 are plotted against $1/\sqrt{c}$ which is approximately equal to the average next-nearest-neighbor distance between the radicals. A linear relationship is found at temperatures below the phase transition ($T < T_t$).

as obtained from the present analysis are shown in Figures 6, 9, and 10.

The temperature dependence of W_{ex} is plotted in Figure 6 for label concentrations between c = 0.035 and c = 0.27. A sharp decrease of W_{ex} is observed in the region between 30 and 40° which is the temperature range of the crystalline–liquid crystalline phase transition of our system (*cf.* introduction to part I). This decrease of W_{ex} with increasing temperature is in complete contrast to the behavior of free radicals in solution.[10,19] It is therefore suggested that this anomalous temperature dependence of W_{ex} indicates a radical change in the organization of the steroid-in-lecithin system at the phase transition.

The proposed structural differences for $T > T_t$ and $T < T_t$ are reflected in a different concentration dependence of W_{ex} for $T > T_t$ and $T < T_t$. In Figure 9 we have plotted W_{ex} as a function of the molar ratio c label:lipid for different temperatures. In Figure 10 W_{ex} is shown as a function of $1/\sqrt{c}$ which is proportional to the average label distance d_{la}. These two figures demonstrate that for $T > T_t$ the exchange frequency increases approximately linearly in c, whereas for $T < T_t$ the relation $W_{ex} = A - B/\sqrt{c}$ is observed.

In part III it will be shown that the data for $T > T_t$ can be analyzed on the basis of a diffusional model in which it is assumed that the steroid molecules can perform translational diffusion within the lipid matrix. The diffusion coefficient D_{diff} is estimated from our measurements as $D_{diff} \approx 10^{-8}$ cm²/sec. The data for $T < T_t$ suggest that the label molecules are practically immobilized with respect to translational diffusion for $T < T_t$ and that the system exhibits a mosaic-like structure in which small clusters of steroid molecules are embedded within the supporting lipid matrix.

(19) J. G. Powles and M. H. Mosley, *Proc. Phys. Soc.*, 78, 370 (1961).